Broadband Wireless Access With Optically Controlled Phased Array Antennas

Guy-Aymar Chakam, Wolfgang Freude

High-Frequency and Quantum Electronics Laboratory (Institut für Hochfrequenztechnik und Quantenelektronik)
University Karlsruhe, Kaiserstr. 12 D-76128 Karlsruhe, Germany
Tel: +49 721 608-2492 Fax: +49 721 608-2786
E-mail: W.Freude@ihq.uni-karlsruhe.de Web: http://www.uni-karlsruhe.de/~ihq

Abstract: *The rapid extension of communication requires systems having higher transmission capacity and lower infrastructure cost than is currently the case. For terrestrial communication, a very promising way is to upgrade existing cables by wireless local area networks using RF carriers in the frequency range* 2.4…60 GHz. *We describe the design of a novel broadband λ-dipole coplanar antenna at 20 GHz using a photonic crystal structure, and we present measured results.*

Existing wired local area networks

Copper pairs and the existing TV cabling allow accessing the Internet far faster than is possible with voice-band modems.

An *a*symmetric *d*igital *s*ubscriber *l*ine (ADSL) may be configured on *p*lain *o*ld *t*elephone *s*ervice (POTS) copper pairs between a subscriber and the first exchange node. In Germany, this `last mile´ has an average length of 2 km, enabling downloads of up to 8 Mbit/s, and uploads with a maximum rate of 768 kBit/s. In the Unites States of America, the `last mile´ amounts to 4.5 km. For this market, a simplified, cheaper version of ADSL is being standardised, named *u*niversal *d*igital *s*ubscriber *l*ine (UDSL). Downloads with 1.5 MBit/s and uploads with 128 kBit/s are sufficient for MPEG-1 video transmission needing a payload of 1.5 MBit/s. *S*ymmetrical single pair DSL (SDSL) systems provides identical up- and downstream rates.

TV cables cover wide areas (10 % of the USA households). Cable modems transmit at a rate of 38 Mbit/s downstream and 2 Mbit/s upstream, such establishing a strong competition to ADSL and UDSL.

However, in many parts of the world the existing POTS or cable wiring is neither good nor dense enough. Optical fibre penetration to commercial buildings and multiple dwelling units is less than 3 % even in industrialised countries.

Wireless local area networks

*W*ireless *l*ocal *a*rea *n*etworks (WLAN) can fill this gap world-wide. Channel capacities of up to 155 Mbit/s are supported for delivering TV signals, high-speed data, and voice telephony. Several frequency bands exist in the range 2.4…60 GHz. For a photonic or TV cable link, the ratio of construction and equipment costs is about 9:1, while it is 2:8 for fixed wireless systems. For WLAN, the cost-to-capacity ratio drops by 50 % every 2.1 years /1/.

Important WLAN standards /2/

WLAN bands at 0.9, 2, 4 and 5 GHz have been available since 1990. In 1997, the international standard IEEE 802.11 specified both *m*edium *a*ccess *c*ontrol (MAC), and three different *phy*sical layers (PHY). Two PHYs are radio-based using the 2.4 GHz band. A third PHY is based on infrared light transmission. All PHYs support a data rate of 1 Mbit/s (optionally 2 Mbit/s). The 2.4 GHz frequency band is available for license exempt use in Europe (output power $P_O \leq$ 100 mW), the USA ($P_O \leq$ 1 W), and Japan ($P_O \leq$ 10 mW).

In 1998, user demand for higher bit rates and international availability of the 2.4 GHz band has spurred the standardisation of a fourth PHY with a basic rate of 11 Mbit/s, supporting also the 1, 2 and 5.5 Mbit/s rates. At the same time, a new 5 GHz standard was defined in the USA, targeting the data rates 6…54 Mbit/s

(*u*nlicensed *n*ational *i*nformation *i*nfrastructure, UNII, $P_O \approx 1$ W).

In Europe, the following standards are currently under consideration: *Hi*gh-*per*formance LAN HiperLAN type 1 (outdoor), type 2 (indoor, 5 GHz band, 20 MHz bandwidth per frequency channel /3/), HiperLink (wireless indoor backbone), HiperAccess (outdoor, fixed WLAN providing access to a wired infrastructure). This is worked out by the *b*roadband *r*adio *a*ccess *n*etworks (BRAN) working group of the *E*uropean *T*elecommunications *S*tandards *I*nstitute (ETSI).

In 1999, the German authorities for Telecommunications Regulation allocated frequencies in the bands 3.5 GHz and 26 GHz to 12 WLAN providers.

In Japan, the Ministry of Post and Telecommunications started standardising indoor WLANs supporting data rates up to 156 Mbit/s using frequencies in the 30…300 GHz band, and high-speed wireless (outdoor) access at 25…30 Mbit/s in the SHF band 3…60 GHz.

Space diversity multiple access

Taking advantage of the spatial dimension in reusing transmission frequencies at appropriate space intervals, i. e., for different radio cells, is a common technique for radio broadcast and cellular telephones. However, multiple-beam antenna arrays tender *s*pace *d*iversity *m*ultiple *a*ccess (SDMA) *within* a single radio cell serving different users on the same frequency channel at the same time /3/. Rather narrow-banded (30 MHz) smart antennas form their beams in the baseband by RF feeding the antenna elements proportional to the appropriately processed baseband signals.

For phased array antennas, beamforming is done at the RF level with *b*eam*f*orming *n*etworks (BFN), which control amplitude and phase of the element feeding signals. To avoid a frequency dependent beam squint for broadband signals, *t*rue *t*ime *d*elay (TTD) BFN are required, where the phase is proportional to the instantaneous RF frequency. For high-frequency carriers above 10 GHz, the only feasible solution in terms of weight, cost and attenuation are *o*ptical BFN (OBFN) with switched optical fibre delay lines. In the following, we discuss the design of a 20 GHz optically fed broadband phased array antenna.

Optically controlled antenna array

Fig. 1 shows a coplanar waveguide (CPW) λ-dipole antenna structure etched on a 104 mm × 81 mm RT Duroid 5880 substrate with a thickness of 1.57 mm, a refractive index of $n \approx 1.5$, and a medium wavelength of $\lambda_n = \lambda/n \approx 10$ mm. The radiating slot length, slot width, and the separation of the dipole elements are $\lambda_n/2 = 5$ mm, 1 mm, and $1.7 \times \lambda_n = 17$ mm, respectively.

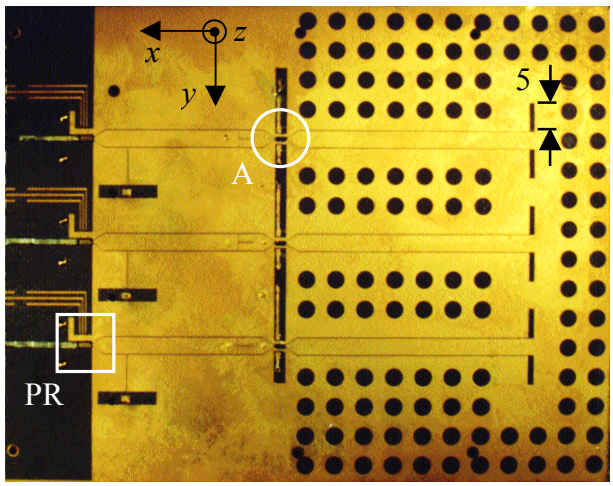

Fig. 1 Optically controlled antenna with photonic crystal structure /4/ /5/, integrated photoreceivers (PR) /7/, and MMIC amplifiers (A)

The photoreceiver (PR) /7/ is grown on a semi-insulating GaAs substrate with chip dimensions 2.5 mm × 1 mm. It includes a pin photodiode (PD) with a circular light-sensitive area of 10 µm diameter, and a six-stage HEMT distributed amplifier with a total gain of 14 dB. At $\lambda = 1.55$ µm, the entire pin-HEMT PR has a transimpedance of 146 Ω corresponding to an O/E conversion factor of 50 V/W, and a bandwidth suitable for NRZ data transmission up to 40 Gbit/s.

Backward radiation is avoided by a back metallization on a Rohacell foam spacer (refractive index 1.025) with a thickness of 5 mm, an arrangement known as a conductor-backed (CB) CPW.

For a structure as in Fig. 1, but in a first step without the circular apertures, we measured

the opto-electronic properties with the following setup. The optical carrier at $\lambda = 1.55$ µm, emitted by a CW DFB laserdiode, was amplitude modulated by a Mach-Zehnder modulator, driven with a sinusoidal 20-GHz RF signal. After propagation through an Erbium-doped fibre amplifier, the modulated light was coupled via standard single-mode fibres to the top-illuminated PD of each of the PR, which detect and amplify the RF signal.

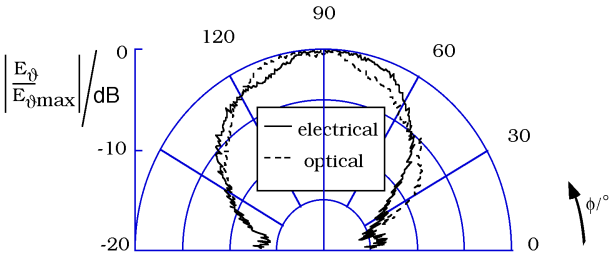

Fig. 2 Radiation pattern of a single antenna element from the structure Fig. 1 at $f = 20$ GHz: Relative magnitude of the electric field E_ϑ in the direction of the x-axis of Fig. 1, measured as a function of angle ϕ in the H-plane (y-z-plane in Fig. 1)

In Fig. 2, the radiation pattern of a single element is displayed, measured in the H-plane (y-z-plane in Fig. 1), both for an all-electric excitation of the antenna, and for an opto-electric feeder as described above.

We also measured the antenna input reflection coefficient $|S_{11}|/\text{dB} = 20\lg|S_{11}|$ of a single antenna element with a provisional electric connector as a function of the RF frequency f, Fig. 4 (·····). The 14-dB bandwidth amounts to 7.5 %. This rather narrow bandwidth is caused by the resonant excitation of parallel plate and surface modes of the CB substrate.

Photonic crystal design

For improving the bandwidth of the CB-CPW structure, we tried to suppress parasitic modes by forming a *p*hotonic *c*rystal (PC) with a *p*hotonic *b*andgap (PBG) /4/–/6/ at the radiation frequency.

As a simple PC design study, we investigated a $L = 250$ mm long microstrip line with holes etched out of the ground plane. The substrate material was RT Duroid 6010 with a 17 µm thick copper metallization, a strip width of 0.56 mm, a refractive index of $n \approx 3.3$ (±1.5 %), and a substrate height 0.635 mm. The holes had a diameter of 6 mm and a spatial period $\Lambda = \lambda_B/(2n_e) = 28.5$ mm corresponding to the vacuum Bragg wavelength λ_B. The field propagates with the effective refractive index n_e. The strip width for the PC structure was chosen to maintain a HE_0 fundamental wave impedance of about 50 Ω. We measured the RF input reflection factor $S_{11}(f)$ and the transmission factor $S_{21}(f)$ of the lines with and without PC grating structure using coaxial 50-Ω equipment.

Further, we computed $S_{11}(f)$ and $S_{21}(f)$ for the microstrip PC structure employing the software package Ensemble Version 6.0 (Ansoft). Measured (– –) and calculated (—) results are displayed in Fig. 3. The computing time using a 450-MHz PIII processor with 768 MB RAM amounted to 2 h for 110 frequency points.

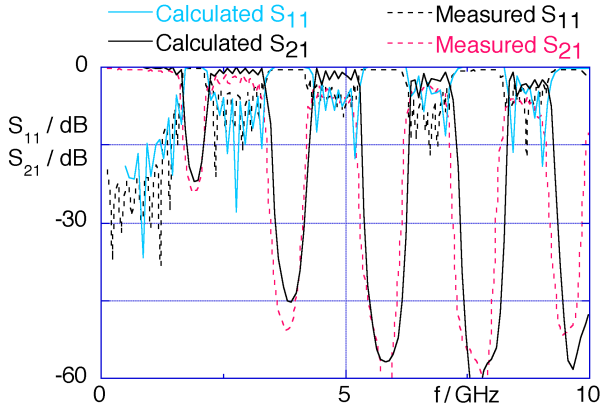

Fig. 3 Measured (– –) and calculated (—) input reflection $|S_{11}(f)|$ and transmission factor $|S_{21}(f)|$. Bragg frequency $f_B = 2.0$ GHz, $f_{min} = 2.3$ GHz

The agreement of measured and computed curves in Fig. 3 is striking. The stop-band is centred at the Bragg frequency $f_B = c/(2n_e\Lambda) = 2.0$ GHz, so that the effective refractive index for wave propagation could be estimated to be $n_e = 2.6$. With the minimum-reflection frequency offset at $f_{min} = 2.3$ GHz, the coupling constant $\kappa = 12\ \text{m}^{-1}$ may be estimated from the well-known relation /8/

$$(f_{min} - f_B)^2 = (\kappa c/(2\pi n_e))^2\,(1 + (\pi/\kappa L)^2).$$

With these data, the maximum power reflection coefficient /8/ for $f = f_B$ and $\kappa L = 3$ can be computed,

$$|S_{11}|^2 = \tanh^2(\kappa L) = 0.99 \quad (-0.04\ \text{dB}).$$

The transmission band power return loss is in the order of $|S_{11}|^2 = 0.03$ (–15 dB).

Waves at multiples p of f_B see the appropriate Fourier component of a p-th order grating. Radiating modes not guided by the strip may be excited /9/, which causes additional stop-band transmission losses and a lower reflection. The radiation mode propagation angles γ as measured from the main propagation direction (strip axis) are /9/

$$\cos \gamma = 1 - 2\, q / p, \qquad q = 0, 1, 2, \ldots$$

PC antenna design

With this experience, we designed the CB-CPW antenna Fig. 1. Waveguides and radiating slots are surrounded by circular apertures etched out of the top metal layer, having a diameter of $0.2 \times \lambda = 0.3 \times \lambda_n = 3$ mm, and thus operating below their resonance frequency. Periodic apertures of the same size are also etched out of the back metallization. The spatial period of the PBG structure equals the length $\lambda/3 = \lambda_n/2 = 5$ mm of the radiating slots.

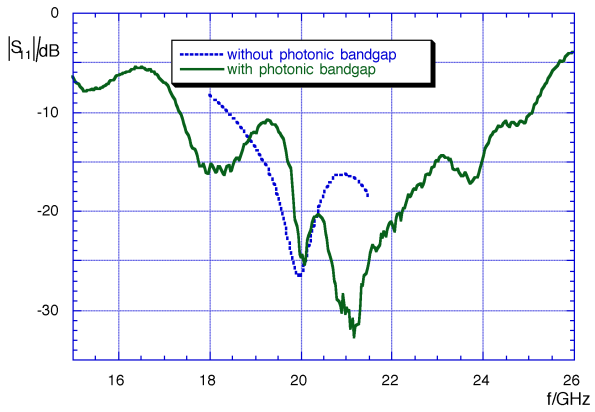

Fig. 4 Modulus of input reflection coefficient $|S_{11}|$ for a single PC antenna element (——) after amplifier A in Fig. 1, and for an equivalent element without PC structure (·····)

We computed the RF input reflection factor $S_{11}(f)$ at the output port of amplifier A in Fig. 1 for a single antenna element, and varied the PC design by trial and error. We employed again the software package Ensemble Version 6.0 (Ansoft). The calculation time using a 450-MHz PIII processor with 512 MB RAM amounted to 36 h for 21 different frequencies.

Measurement results are to be seen in Fig. 4 (—). The 14-dB bandwidth of our PC antenna tripled from 7.5 % to 22 % (4.4 GHz).

Conclusion

Beam squint of broadband phased array antennas can be avoided by optical true time delay beamformers. By switching this network, one ore multiple beams may be steered. We designed a coplanar phased array λ-dipole antenna with optical feeder and photonic crystal structure, and investigated the system using an external light modulator. At $f = 20$ GHz we measured a large relative bandwidth of 22 % (4.4 GHz). The components allow a design scaling to $f \approx 40$ GHz.

Acknowledgement Thanks are due to W. Wiesbeck from Microwaves and Electronics Laboratory, University Karlsruhe, for providing measurement and software resources. We thank V. Hurm and H. Walcher from Fraunhofer Institute for Applied Solid-State Physics, Freiburg, for supplying the photoreceivers and for help with the chip mounting. – This work was supported by Ministerium für Wissenschaft, Forschung und Kunst Baden Württemberg ("Nanotechnologie", Az. 24-7532.23-5-14/4 - 06.04.1998)

References

/1/ Dutta-Roy, A.: Fixed wireless routes for Internet access. IEEE Spectrum Sept. (1999) 61–69

/2/ van Nee, R.; Awater, G.; Morikura, M.; Takanashi, H.; Webster, M.; Halford, K. W.: New high-rate wireless LAN standards. IEEE Comm. Mag. 37 (1999) No. 12, 82–88

/3/ Vornefeld, U.; Walke, C.; Walke, B.: SDMA techniques for wireless ATM. IEEE Comm. Mag. 37 (1999) No. 11, 52–57

/4/ Chakam, G.-A.; Freude, W.: Koplanare Schlitzantenne mit Photonic-Bandgap-Struktur. Patent pending at Deutsches Patentamt München, Az. 199 55 205.3, 17. Nov. 1999

/5/ Chakam, G.-A.; Freude, W.: Coplanar phased array antenna with optical feeder and photonic bandgap structure. Post-Deadline Papers Intern. Topical Meeting on Microwave Photonics MWP'99, Melbourne, 17.–19. Nov. 1999, pp. 1–4

/6/ Scherer, A. et al.: Special issues on electromagnetic crystal structures, design, synthesis, and applications. **(a)** J. Lightwave Technol. 17 (Nov. 1999) 1928 ff. **(b)** IEEE Microwave Theory Tech. 47 (Nov. 1999) 2057 ff.

/7/ Hurm, V. at al.: 40 Gbit/s 1.55 µm monolithic integrated GaAs-based PIN-HEMT photoreceiver. Proc. 24th Europ. Conf. Opt. Commun. Madrid (ECOC'98), Vol. 3, 121-123, 1998

/8/ Ebeling, K. J.: Integrierte Optoelektronik, 2nd Ed. Berlin: Springer 1992. Eq. (5.17), (5.14)

/9/ Hunsberger, R. G.: Integrated optics, 4th Ed. Berlin: Springer 1995. Eq. (13.1.13)